CrystEngComm

Accepted Manuscript

Volume 18 | Number 1 | 7 January 2016 | Pages 1–184

CrystEngComm

www.rsc.org/crystengcomm

ROYAL SOCIETY OF CHEMISTRY

HIGHLIGHT
Tiddo J. Mooibroek, Antonio Frontera et al
Towards design strategies for anion–π interactions in crystal engineering

175 YEARS

This is an Accepted Manuscript, which has been through the Royal Society of Chemistry peer review process and has been accepted for publication.

Accepted Manuscripts are published online shortly after acceptance, before technical editing, formatting and proof reading. Using this free service, authors can make their results available to the community, in citable form, before we publish the edited article. We will replace this Accepted Manuscript with the edited and formatted Advance Article as soon as it is available.

You can find more information about Accepted Manuscripts in the author guidelines.

Please note that technical editing may introduce minor changes to the text and/or graphics, which may alter content. The journal's standard Terms & Conditions and the ethical guidelines, outlined in our author and reviewer resource centre, still apply. In no event shall the Royal Society of Chemistry be held responsible for any errors or omissions in this Accepted Manuscript or any consequences arising from the use of any information it contains.

ROYAL SOCIETY OF CHEMISTRY

ROYAL SOCIETY
OF CHEMISTRY

Journal Name

COMMUNICATION

From Diiodo Tröger's Bases Towards Halogen-Bonded Porous Organic Crystalline Materials

Lucía González,[a,b] Sara Graus,[c] Rosa María Tejedor,[d] Pilar López,[a] José Elguero,[e] José Luis Serrano,[a,f] Santiago Uriel.[g*]
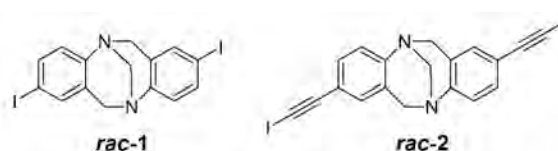
Racemic 2,8-diiodo-6H,12H-5,11-methanodibenzodiazocine (*rac-1*) and racemic 2,8-diiodoethynyl-6H,12H-5,11-methano-dibenzodiazocine (*rac-2*) proved to be self-complementary tectons that are particularly suitable for the formation of porous supramolecular structures by halogen bonding. Crystals structures of clathrate *rac-1·CH₂Cl₂* and *rac-2* show channels, which represent 20% of the cell volume, and these are stabilized by strong C–I···N and C–I···π(Ar) halogen bonds.

One of the most important challenges in materials science is to obtain well-defined supramolecular topologies in order to optimize the physical properties inherent in these structures.[1,2] Nevertheless, due to the weak intermolecular interactions involved in supramolecular chemistry it is very difficult to predict a priori the macroscopic orientation that will be obtained. This situation is particularly acute in the case of crystal engineering because almost insignificant changes in the molecule can lead to the formation of very different crystal structures.[3,4]

The synthesis and characterisation of porous materials have become a hot research area in materials science and particularly in crystal engineering.[5,6] In this context, porous organic crystalline materials (POCM's), which have lower densities than the porous materials such as zeolites and metal-organic frameworks (MOFs), have attracted increased research interest in recent years.[7,8,9,10] In this line of research the

geometry of the molecules involved and the interactions promoted by their active groups play a fundamental role in defining the crystal structure obtained.[14] In this respect, one structure that is of particular interest is Tröger's base (TB) because its almost 90º angular geometry and rigid conformation are especially suited to form different types of polygonal structures that can contain a cavity.[13,14] Indeed, organic nanoporous polymers containing bicovalently bonded Tröger's base in the network with a high BET surface[15,16,17,18] have been described. Furthermore, in recent years the halogen bonding interaction has proven to be particularly useful in supramolecular chemistry.[19,20] More specifically, a number of POCM's based on halogen bonding have been described.[21,22] We describe here the combination of Tröger's base analogues and halogen bonding to obtain porous crystalline materials that exploit the geometry and self-complementarity of diiodo-Tröger's base derivatives. We selected racemic 2,8-diiodo-6H,12H-5,11-methanodibenzo-diazocine (rac-1) and racemic 2,8-diiodoethynyl-6H,12H-5,11-methanodibenzodiazocine (rac-2) (See Chart 1) as key materials.

The electron density map of diiodo Tröger's base analogues

rac-1   rac-2

shows two electron density donor groups (nitrogen atoms) and two electron density acceptors (iodine atoms) with a pseudo-tetrahedral distribution that gives rise to heterotopic AX₂Y₂ tectons (Figure 1). To date, only two crystal structures have been described for these tecton types that can bind through halogen bonds with a tetrahedral arrangement of functional groups, namely 4,4-dinitro-4',4"-diiodotetraphenylmethane[23] and the *5S,11S* enantiomer of a 2,8-diiodo Tröger's base derivative.[24] In fact the crystal structure of the latter compound, described by Wärnmark and coll., contains

a. Departamento de Química Orgánica, Facultad de Ciencias, Universidad de Zaragoza, 50009 Zaragoza (Spain).
b. Instituto de Ciencia de Materiales de Aragón, Universidad de Zaragoza–CSIC, 50009 Zaragoza (Spain).
c. Departamento de Química Física, Facultad de Ciencias, Universidad de Zaragoza, 50009 Zaragoza (Spain).
d. Centro Universitario de la Defensa, Academia General Militar, 50090 Zaragoza (Spain).
e. Instituto de Química Médica, IQM-CSIC, 28006 Madrid (Spain).
f. Instituto de Nanociencia Aragón, Universidad de Zaragoza, 50018 Zaragoza (Spain).
g. Departamento de Química Orgánica, Escuela de Ingeniería y Arquitectura, Universidad de Zaragoza, 50018 Zaragoza (Spain).
† Electronic supplementary information (ESI) available. Synthesis, characterization and computational details. CCDC 1023121-1023123 and 1822048. For ESI and crystallographic data in CIF or other electronic format see DOI: 10.1039/x0xx00000x

CrystEngComm Accepted Manuscript

COMMUNICATION

channels, in which the solvent is located, formed by C–I···π$_{(Ar)}$ halogen bonding.

We decided to use racemic mixtures to synthesize **rac-2** because in the crystal structures of iodo Tröger´s base derivatives formed by a single enantiomer, as reported in the Cambridge Structure Database, the acceptor in the halogen bonding is the electron density of the aromatic rings.[24,25] In contrast, in derivatives that contain the pair of enantiomers it is the nitrogen atoms that act as halogen bonding acceptors.[26] Compound **rac-2** was prepared in an effort to increase the magnitude of the iodine σ-hole. The V$_{s,max}$ of **rac-2** is 23.5 kcal/mol, as shown in Figure 1, and this is significantly higher than that of **rac-1** (10.8 kcal/mol) and similar to those of strong XB donors such as 1,4-bis(iodoethynyl)benzene (25.2
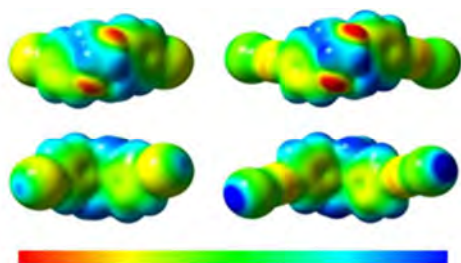

Figure 1. Computed electrostatic potentials of the minimized geometries of **rac-1** (left) and **rac-2** (right). Potentials are mapped on the respective electron density isosurfaces (0.002 a.u.). Electrostatic potential values range from −0.04 (red) to 0.04 (blue).

kcal/mol) and 1,4-diiodo-tetrafluorobenzene (25.9 kcal/mol). The electrostatic potential values for iodine atoms in **rac-1** and **rac-2** indicate that the hybridization of the carbon atom adjacent to the halogen bonded atom has a marked influence on the maximum value of the electrostatic potential. Moreover, assuming that most conventional halogen bonding interactions are dominated by electrostatic factors, the most effective XB-donor with a suitable XB-acceptor should lead to more favorable halogen bonding, i.e., the contribution of the Lewis base to σ-hole bonding is usually significant. Thus, **rac-2** combines the most effective XB-donor and the most effective XB-acceptor (V$_{s,min}$ = −19.6 kcal/mol) of the two molecules studied here.[27] In addition, the rigid extended linear nature of the iodoethynyl group improve iodine accessibility, which makes the iodoethynyl group very useful in crystal engineering. Although haloalkynes have a well-established role in synthetic organic chemistry,[28] their application in supramolecular chemistry is less well developed despite their long history.[29,30,31]

Crystals of clathrate **rac-1·CH$_2$Cl$_2$** were obtained by crystallization of **rac-1** from a dichloromethane solution. This clathrate crystallizes in the orthorhombic system and was solved in the non-centrosymmetric Iba$_2$ space group. The asymmetric unit has two **rac-1** (lying about twofold axes), and a dichloromethane molecule in a general position. The supramolecular arrangement is determined by the halogen

bonds C(1)–I(1)···N(2a) (3.13 Å 172.4°) and C(10)–I(2)···N(1b) (3.22 Å 159.3°) (See Table S2 in the Supporting Information). The halogen bonding distances are 11 and 9% shorter than the sum of the van der Waals radii of N and I (3.53 Å). The interaction energies of optimized **rac-1·CH$_2$Cl$_2$** dimers corrected for the Basis Set Superposition Error (ΔE$_{BSSE}$) were determined to be −6.89 and −6.78 kcal/mol (halogen bonded dimers, the interaction energy and key geometric parameters are gathered in Tables S4 and S5 in the Supporting Information). Each 2,8-diiodo TB molecule acts as a heterotopic tetradentate building block surrounded by four molecules in a distorted tetrahedral environment (Figure 2(a), which gives rise to a diamond-like network. Overall the
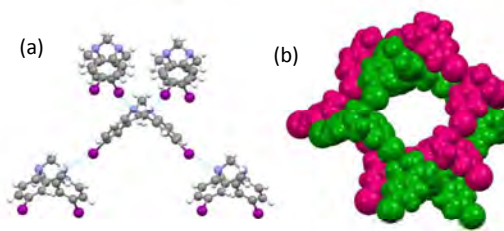

Figure 2. Crystal structure of solvate **rac-1·CH$_2$Cl$_2$**. (a) Adamantanoid arrangement and interpenetrated diamond networks (b).

structure has two interpenetrated diamondoid nets (red and green in Figure 2(b)) to form channels along the c axis, with dichloromethane molecules located within these channels.

Each of these virtual channels, regardless of the presence of dichloromethane, has a volume of 209 Å^3 per unit cell, which represents 23.7% of the cell volume. The structure can also be described (Figure 3) as channels formed by a pseudo-helical arrangement of the two enantiomers through halogen bonds. Crystals of **rac-1·CH$_2$Cl$_2$** lose crystallinity quickly when they are removed from their mother liquor. This evolution could be due
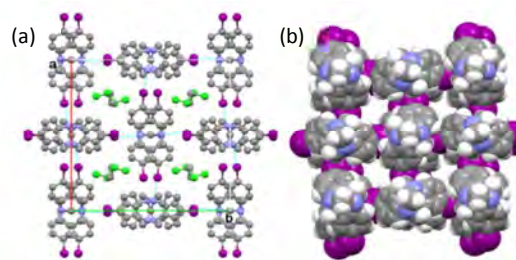

Figure 3. Crystal structure of solvate **rac-1·CH$_2$Cl$_2$**. (a) Channel along the c axis with CH$_2$Cl$_2$ molecules. (b) View of channels in which solvent molecules have been omitted.

to the inherent instability of clathrates with a diamond-like structure and to the weakness, in this case, of halogen bonds. This weakness is manifested in the small reduction in the C–I···N distance with respect to the sum of the VdW radii (ca. 10%) and is due to the small magnitude of the σ-hole.[32]

Journal Name COMMUNICATION

The XRD pattern of **rac-1·CH₂Cl₂** crystals taken from the mother liquor resembles the calculated powder diffractogram of the more compact structure **rac-1** (Figure S1). Condensed phases of **rac-1** and of enantiomerically pure **(5S,11S)-1** were successfully crystallized from toluene solutions. Although **rac-1** and **(5S,11S)-1** crystallized in monoclinic and triclinic systems, respectively, both structures have two independent molecules in their asymmetric units and their supramolecular organizations show some similarities. In both cases the molecules stack along the *a* axis. In **rac-1** the stacks are formed by two interdigitated homochiral strings rotated with respect to one another by 45.6° [Figure 4(a)] while in **(5S,11S)-1** the stacks are formed by face-to-face offset dimers, in which the
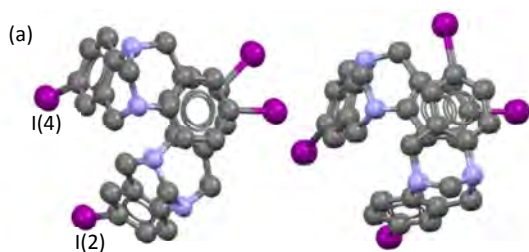

Figure 4. Detail of the stacks along the *a* axis in the **rac-1** and **(5S, 11S)-1** crystal structures.

molecules are rotated by 102.8° relative to one another (Figure 4(b)).

The supramolecular arrangement of **rac-1** is formed by ac planes. On the surface of these planes are iodine atoms I(1) and I(3), which do not interact, and this isolates the planes from each other along the *b* axis (Figure 5(a)). Moreover, I(4) and I(2) act as XB donors in C–I(4)···I(2) (3.86 Å, 173°) and C–I(2)···N(11) (3.16 Å, 163°) interactions. Accordingly, I(2) acts as a halogen bonding donor and acceptor, as depicted in Figure 5(b).

The stacks in **(5S,11S)-1** are connected along the *b* axis by halogen···halogen C–I···I (3.88 Å, 162.4°) halogen bonding. It should be noted that both the **rac-1** and **(5S, 11S)-1** structures contain C–I···I halogen bonds. These are the first examples of such interactions in Tröger's base derivatives and they highlight the versatility of halogen bonding to form novel supramolecular organizations. Additionally, the intermolecular
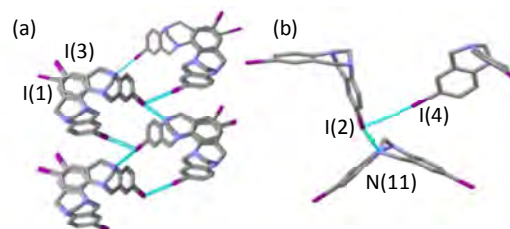

Figure 5. (a) Halogen bond network in the crystal structure **rac-1**, (b) Detail of C–I···I and C–I···N halogen bonds in **rac-1**.

contacts in **rac-1·CH₂Cl₂, rac-1 and (5S,11S)-1** crystal structures were analyzed by Hirshfeld surfaces (Figures S2 and S3).

In an effort to overcome the instability observed in the **rac-1·CH₂Cl₂** structure, we synthesized **rac-2** from **rac-1** in two steps. The first step was a Sonogashira coupling with trimethylsilylacetylene[33,34] and the second involved treatment with N-iodosuccinimide and silver nitrate in dimethylformamide.

The crystal structure of **rac-2** was solved in the monoclinic P2₁/c space group and its asymmetric unit consists of one molecule in a general position. The first consequence of the introduction of iodoethynyl groups is an increase in the distance between the iodine atoms, which changes from about 10 Å in **rac-1** to 13.3 Å in **rac-2**. The second consequence is that the halogen bonding distance C–I···N (2.80 Å) is shorter than in the structures of **rac-1·CH₂Cl₂** (3.13 and 3.22 Å) and **rac-1** (3.16 Å). This difference is due to the higher electron-withdrawing effect of *sp* iodo-carbon hybridization and the lower temperature employed in data collection. The **rac-2** supramolecular organization can be described starting from racemic dimers formed by two C–I···$\pi_{(Ar)}$ (3.474 Å) halogen bonds [Figure 6(a)]. Similar dimers have been described in 2,8-dibromo Tröger's base structure with C–Br···$\pi_{(Ar)}$ (3.488 Å) halogen bondings.[35] The C–I···$\pi_{(Ar)}$ dimers interact by C_{sp}–I···N halogen bonds (2.80 Å, 172.7°), which result in planar distorted hexagonal net with a distance between opposite sides of 15 and 19 Å. [Figure 6(b)]. The stabilization energies of the C–I···$\pi_{(Ar)}$ and C_{sp}–I···N halogen bonds were calculated as −15.77 (per dimer) and −8.95 kcal/mol, respectively (Figure S4 and Tables S4 to S6 in the Supporting Information).
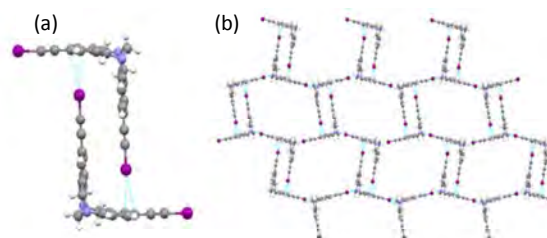
This journal is © The Royal Society of Chemistry 20xx

Figure 6. Crystal structure of **rac-2**: (a) Halogen bonded dimer; (b) planes formed by dimers through C–I···N halogen bonding.

3

COMMUNICATION

Journal Name

The planes, which are related by a center of inversion, are assembled by weak C_{sp3}–H···π(alk) hydrogen bonding (Table S3 in the Supporting Information) and π···π stacking between dimers [Figure 7(a)]. These two-dimensional aggregates are stacked, which leads to channels along the c axis that represent 20% (417.51 Å^3) of the unit cell volume,
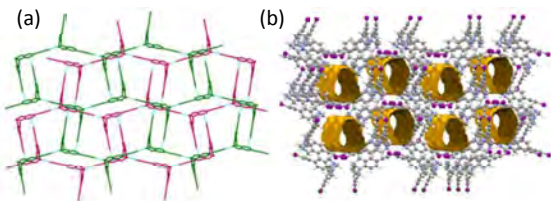

Figure 7. Crystal structure of **rac-2**: (a) aggregate formed by two planes related by an inversion center (b) voids in the halogen and hydrogen bonding 3D network along the a axis.

[Figure 7(b)]. Residual electron density peaks observed inside the channels were refined as 0.4 molecules of dichloromethane per 2,8-diiodoethynyl Tröger's base molecule as a rigid group that pivots around one of the chlorine atoms.

In summary, we have demonstrated that diiodo Tröger's base derivatives **rac-1** and **rac-2** are chiral tetraheterotopic self-complementary building blocks that are suitable to obtain porous organic crystalline materials. The versatility of halogen bonding to obtain novel supramolecular organizations has also been exemplified. Thus, we obtained an unstable porous diamondoid-type structure, based on C–I···N halogen bonds, on crystallizing **rac-1** from a dichloromethane solution. The instability was overcome by replacing the iodine atoms with iodo-ethynyl groups. These groups form strong halogen bonds, improve iodine accessibility and increase the Tröger's base cleft. The crystal structure of **rac-2** shows channels that represent 20% of the cell volume.

Conflicts of interest

There are no conflicts to declare.

Notes and references

1   X. Wang, D. S. Miller, E. Bukusoglu, J. J. De Pablo and N. L. Abbott, *Nat. Mater.*, 2016, **15**, 106–112.
2   P. Schönherr, S. Zhang, Y. Liu, P. Kusch, S. Reich, T. Giles, D. Daisenberger, D. Prabhakaran, Y. Chen and T. Hesjedal, *Phys. Status Solidi*, 2015, **9**, 130–135.
3   A. Bajpai, M. Lusi and M. J. Zaworotko, *Chem. Commun.*, 2017, **53**, 3978–3981.
4   O. K. Farha, C. D. Malliakas, M. G. Kanatzidis and J. T. Hupp, *J. Am. Chem. Soc.*, 2010, **132**, 950–952.
5   H. Furukawa, K. E. Cordova, M. O'Keeffe and O. M. Yaghi, *Science (80-.).*, 2013, **341**, 1230444.
6   P. J. Waller, F. Gándara and O. M. Yaghi, *Acc. Chem. Res.*, 2015, **48**, 3053–3063.
7   N. B. McKeown, *J. Mater. Chem.*, 2010, **20**, 10588–10597.
8   J. R. Holst, A. Trewin and A. I. Cooper, *Nat. Chem.*, 2010, **2**, 915–920.
9   Y. Sheng, Q. Chen, J. Yao, Y. Lu, H. Liu and S. Dai, *Angew. Chem. Int. Ed.*, 2016, **55**, 3378 –3381.
10   X. Huang, Y.-C. Zhao and B.-H. Han, *Chem. Commun.*, 2016, **52**, 6597–6600.
11   T. R. Cook, Y. R. Zheng and P. J. Stang, *Chem. Rev.*, 2013, **113**, 734–777.
12   T. R. Cook and P. J. Stang, *Chem. Rev.*, 2015, **115**, 7001–7045.
13   S. Sergeyev, *Helv. Chim. Acta*, 2009, **92**, 415–444.
14   Ö. V. Rúnarsson, J. Artacho and K. Wärnmark, *Eur. J. Org. Chem.*, 2012, 7015–7041.
15   X. Du, Y. Sun, B. Tan, Q. Teng, X. Yao, C. Su and W. Wang, *Chem. Commun.*, 2010, **46**, 970–972.
16   M. Carta, R. Malpass-Evans, M. Croad, Y. Rogan, J. C. Jansen, P. Bernardo, F. Bazzarelli and N. B. McKeown, *Science (80-.).*, 2013, **339**, 303–307.
17   M. Carta, M. Croad, R. Malpass-Evans, J. C. Jansen, P. Bernardo, G. Clarizia, K. Friess, M. Lanč and N. B. McKeown, *Adv. Mater.*, 2014, **26**, 3526–3531.
18   Z.-Z. Yang, H. Zhang, B. Yu, Y. Zhao, G. Ji and Z. Liu, *Chem. Commun.*, 2015, **51**, 1271–1274.
19   P. Metrangolo, F. Meyer, T. Pilati, G. Resnati and G. Terraneo, *Angew. Chem. Int. Ed.*, 2008, **47**, 6114 – 6127.
20   L. C. Gilday, S. W. Robinson, T. A. Barendt, M. J. Langton, B. R. Mullaney and P. D. Beer, *Chem. Rev.*, 2015, **115**, 7118–7195.
21   K. Raatikainen, J. Huuskonen, M. Lahtinen, P. Metrangolo and K. Rissanen, *Chem. Commun.*, 2009, 2160–2162.
22   K. Raatikainen and K. Rissanen, *Chem. Sci.*, 2012, **3**, 1235–1239.
23   R. Thaimattam, C. V. K. Sharma, A. Clearfield and G. R. Desiraju, *Cryst. Growth Des.*, 2001, **1**, 103–106.
24   C. S. Arribas, O. F. Wendt, A. P. Sundin, C.-J. Carling, R. Wang, R. P. Lemieux and K. Wanmark, *Chem. Commun.*, 2010, **46**, 4381–4383.
25   C. Benkhäuser-Schunk, B. Wezisla, K. Urbahn, U. Kiehne, J. Daniels, G. Schnakenburg, N. Frank and A. Lützen, *Chempluschem*, 2012, **77**, 396 – 403.
26   M. Faroughi, K. X. Zhu, P. Jensen, D. C. Craig and A. C. Try, *Eur. J. Org. Chem.*, 2009, 4266–4272.
27   C. B. Aakeröy, M. Baldrighi, J. Desper, P. Metrangolo and G. Resnati, *Chem. Eur. J.*, 2013, **19**, 16240–16247.
28   W. Wu and H. Jiang, *Acc. Chem. Res.*, 2014, **47**, 2483–2504.
29   H. M. Yamamoto, Y. Kosaka, R. Maeda, J. I. Yamaura, A. Nakao, T. Nakamura and R. Kato, *ACS Nano*, 2008, **2**, 143–155.
30   A. Sun, *Science (80-.).*, 2006, **312**, 1030–1033.
31   J. Lieffrig, O. Jeannin and M. Fourmigué, *J. Am. Chem. Soc.*, 2013, **135**, 6200–6210.
32   P. Politzer, P. Lane, M. C. Concha, Y. Ma and J. S. Murray, *J.*

CrystEngComm

COMMUNICATION

Mol. Model, 2007, **13**, 305–311.

33   J. Jensen, M. Strozyk and K. Wärnmark, *Synthesis (Stuttg).*, 2002, 2761–2765.

34   U. Kiehne and A. Lutzen, *Synthesis (Stuttg).*, 2004, 1687–1695.

35   M. Faroughi, A. C. Try and P. Turner, *Acta Crystallogr., Sect. E Struct. Rep. Online*, 2006, **62**, o3674–o3675.

CrystEngComm Accepted Manuscript